Available online at www.sciencedirect.com

ScienceDirect

International Journal of Pavement Research and Technology xxx (2016) xxx–xxx

www.elsevier.com/locate/IJPRT

Use of image analysis for the evaluation of rolling bottle tests results

Claudio Lantieri, Riccardo Lamperti *, Andrea Simone, Valeria Vignali, Cesare Sangiorgi, Giulio Dondi, Michele Magnani

DICAM Department, School of Engineering and Architecture, University of Bologna, Viale Risorgimento 2, 40136 Bologna, Italy

Received 20 May 2016; received in revised form 31 October 2016; accepted 11 November 2016

Abstract

The adhesion between bitumen and aggregates is of paramount importance for asphalt mixtures, because it is confirmed that a weak bond strength results in a premature failure of the pavement. Methods for determining the affinity or the adhesion between components are made both on loose and compacted samples.

Among the first category the rolling bottle method, which is standardized in EN 12697-11 part a, is very common. It represents a simple, rapid and low cost test for an indication of the affinity between aggregate and bitumen and its influence on the susceptibility of the mixture to stripping.

This paper proposes the use of 2D image analysis to evaluate the rolling bottle test results, overcoming the limits and shortcomings of the visual analysis prescribed by the reference standard.

In order to demonstrate its applicability to a broad range of materials, this procedure was applied to both light and dark aggregates, mixed with a wax modified binder. The mixing temperature was varied so that the influence of the binder viscosity on the adhesion was assessed.

A comparison between visual and semi-automatic estimation is presented, demonstrating that the latter brings to far better results. The accuracies were determined through confusion matrixes that permit to identify the errors made during the process of classification.

1. Introduction

Asphalt mixture is a complex and heterogeneous material that includes aggregates, asphalt binder and air voids. Its overall mechanical response is primarily governed by the asphalt binder and by the stone-on-stone contacts between aggregates [5,6,21,22].

Moisture damage is a very complex mode of asphalt mixture distress that leads to the loss of stiffness and structure strength of the asphalt pavement layers and eventually the failure of the road structure [1].

Presence of moisture in the pavement can result in the loss of cohesion within the bituminous binder itself or more often of interfacial adhesion between binder and the aggregates [23].

Moreover, although not all damage is caused directly by moisture, its presence increases the extent and severity of already existing distresses like cracking, potholes, and rutting [17].

Many variables affect the rate of moisture damage, which occurs in an asphalt mixture. Some of them are related to the constituent materials such as aggregate (physical characteristics, composition, dust and clay

* Corresponding author.
E-mail addresses: claudio.lantieri2@unibo.it (C. Lantieri), riccardo.lamperti2@unibo.it (R. Lamperti), andrea.simone@unibo.it (A. Simone), valeria.vignali@unibo.it (V. Vignali), cesare.sangiorgi4@unibo.it (C. Sangiorgi), giulio.dondi@unibo.it (G. Dondi), michele.magnani@studio.unibo.it (M. Magnani).
Peer review under responsibility of Chinese Society of Pavement Engineering.

http://dx.doi.org/10.1016/j.ijprt.2016.11.003

coatings) and bitumen (chemical composition, grade, hardness, crude source and refining process). Others are related to mixture design and layer construction (air voids content, film thickness, permeability and drainage) or environmental factors (temperature, pavement age, freeze–thaw cycles and presence of ions in the water) [4,9].

In order to assess the moisture effects on asphalt concretes, the research works are divided into tests on compacted or loose samples. The first category involves the evaluation of mechanical properties by tensile tests [23] or by determination of the water sensitivity of bituminous specimens according to EN 12697-12 [8], or by combined aging/moisture sensitivity laboratory test according to EN 12797-45 [3,14].

The second involves the study of the compatibility of the binders to the aggregate, focusing on to interfacial tension relations of the materials involved [11,2,15,16].

The standardized European approach to quantify the affinity between aggregate and bitumen is the rolling bottle test [7]. It consists in placing bitumen-coated aggregates in a bottle filled with de-ionized water and then placing it in a rolling machine, which subjects the material to a mechanical stirring action in the presence of water. After defined time steps, normally 6 and 24 h, two independent operators visually estimate the residual degree of bitumen coverage of the particles. Despite being a rapid, simple and low cost test, results may be altered by a large amount of factors, because the determination of the bitumen coverage degree is inevitably subjective. The main factors that may influence the estimation are linked to the operators' skills, the light conditions and the color of the aggregates. Dark or gray aggregates like basalt or blast furnace slag may be confused with bitumen [15,16].

Recently, with the development of new technologies, different attempts were performed in order to improve the determination of the degree of bitumen coverage of aggregates after the rolling bottle test.

Grönniger et al. [10] proposed the use of a computer aided analysis technique based on digital imaging of the binder-coated aggregate-particles after the rolling process, and on classification of characteristic color areas using a commercial computer software.

Mulsow [18], based on the observation that the microroughness of the surface of the aggregate is significantly higher than bitumen, studied the adhesion with a multidirectional reflectance measurement.

Källén et al. [13] compared two methods for the degree of bitumen coverage determination. The first one estimates it by segmenting the image into bitumen and stone and counting the number of pixels accordingly. The second method, instead, uses the amount of specular reflections that occur in the image. In order to do that several images with light from different directions are needed so that reflections occur in one or more of the images but not in the others.

This paper proposes the use of 2D image analysis to evaluate the results of the rolling bottle tests, overcoming the limits and shortcomings of the visual analysis prescribed by the reference standard.

The accuracy of the proposed procedure is validated through a pixel inspection that resulted in confusion matrices for the assessment of errors indexes. A comparison between visual and semi-automatic estimation is presented, demonstrating that the latter brings to far better results.

The materials investigated are three different colored aggregates mixed with wax modified binders. The mixing temperature was varied so that the influence of the binder viscosity on the adhesion was also assessed.

2. Experimental procedure

2.1. Rolling bottle tests

The image analysis procedure proposed in this paper aims at improving the determination of the degree of bitumen coverage after rolling bottle test.

The tests were run at a temperature of 20 °C ± 1 °C with a rolling speed of 60 rpm, while the rolling time was set to 6 h and 24 h. At every stage, three independent operators made visual observations and digital images were taken.

To facilitate the determination of the degree of bitumen coverage over the aggregates both for visual observation and semi-automatic evaluation, the sample was placed on a plate filled with de-ionized water which was laid on a green background. The pictures were taken vertically from a distance of 18 cm, with a 10 Megapixels camera set to ISO 100 (which indicates the camera's sensitivity to light). Two lamps with an angle of incidence of the light beam of 45°, to avoid reflections and to decrease the shadows of aggregates, illuminated the plate. Each lamp had a luminous flux of 70 lm, led white warm light (2.700 of the Kelvin scale). Fig. 1 shows the equipment used to take the pictures.

2.2. Image analysis methodology

The pictures were analyzed with ImageJ, an open source image-processing program.

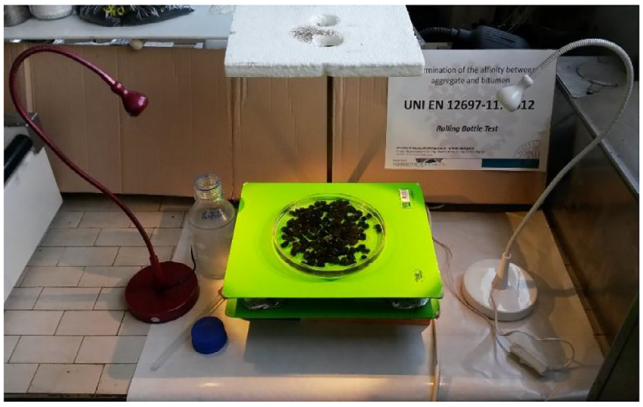

Fig. 1. Set for digital picturing of tested samples.

Please cite this article in press as: C. Lantieri et al., Use of image analysis for the evaluation of rolling bottle tests results, Int. J. Pavement Res. Technol. (2016), http://dx.doi.org/10.1016/j.ijprt.2016.11.003

For the determination of the degree of coverage of bitumen, the analyzed pictures underwent a process where the pixels were classified based on their YUV value. The Y component refers to the luminance of the color, and the U and V components determine the color itself, i.e. the chromaticity [12]. The ability to classify the pixels in function of their color was possible through a specific plugin inside ImageJ. This plugin allows the interaction with the single components of different color space and highlights certain kinds of colors more than others. The YUV color space was chosen for the classification for its better capability to classify the pixels, especially for the isolation of the background and the reduced cutting of the aggregate border. The color space YUV is similar to RGB regarding the concept of additivity, but the components characterizing the model are very different.

Once the original picture (Fig. 2a) is loaded in ImageJ, the first step is to eliminate the background by setting a specific value of the Y, U and V components. In this way a *non-classified image* is saved, representing bitumen and aggregates (Fig. 2b). The second step was to eliminate the color component, which represented the aggregate, and to identify the so-called *classified image*. Similarly to the first step, a specific combination of Y, U and V components is set so that the aggregate pixels are eliminated and only the bitumen remains (Fig. 2c). Then the pixel area of bitumen is calculated.

An ImageJ function makes it possible to calculate the pixel area of pictures. Accordingly, the percentage of the bitumen coverage of the aggregates is then calculated through Eq. (1), where $A_{bitumen}$ refers to the total area of bitumen coverage and $A_{bitumen+aggregates}$ refers to the total area of coated and stripped aggregates:

$$Bitumen\ coverage = \frac{A_{bitumen}}{A_{bitumen+aggregates}} \times 100\ [\%] \quad (1)$$

2.3. Procedure validation

After the classification process, the accuracy of the calculated bitumen coverage was evaluated on a first series of rolling bottle tests performed on the investigated aggregates. In fact, the processes to eliminate the background and the aggregates were done manually. For the evaluation, a specific Java-based code was written, in order to superimpose a 51×51 grid of equidistant points on both the *non-classified* and *classified image* and to extract their RGB average values and x,y coordinates [15,16]. Firstly the RGB average values and x,y coordinates were extracted from the *non-classified image*. Then through a visual observation an operator assigned each pixel to one of the three classes: background, aggregates and bitumen. The process was repeated on the *classified image* and the pixels were classified as background or bitumen in function of the RGB average values extracted. In this case only two classes are used because the *classified image* does not contain aggregates.

The pixels' classification was then used for the construction of confusion matrices (or dispersion matrices). The confusion matrix has many rows and columns as the classes allowing calculations on the accuracy of the classification. Four different accuracy indexes were calculated, according to Table 1.

Tables 2–4 show the confusion matrixes of the tested aggregates and their accuracy indexes. "bkGD" stands for background, "Bit." stands for bitumen, while "B", "L" and "P" stand for the three different aggregates (basalt, limestone and porphyry). The tables can be read in two directions: horizontally and vertically. For example, the vertical reading of Table 2 highlights that 5 out of the 209 total pixels of limestone were classified as bitumen; 17 out of the 546 total pixels of bitumen were classified as limestone; 10 out of the 1846 total pixels of background were classified as limestone (2 pixels) and bitumen (8 pixels). The horizontal reading of Table 2, instead, highlights that 19 out of 223 total pixels were classified by the software as limestone, but actually are bitumen (17 pixels) and background (2 pixels); 13 out of 542 total pixels classified by the software as bitumen actually are limestone (5 pixels) and background (8 pixels). The tables show how User's Accuracy of limestone (91.5%) and porphyry (97.7%) is more accurate than basalt one (88.7%). The same observation can be made for the Producer's Accuracy: the limestone (97.6%) and porphyry (96.6%) is more accurate

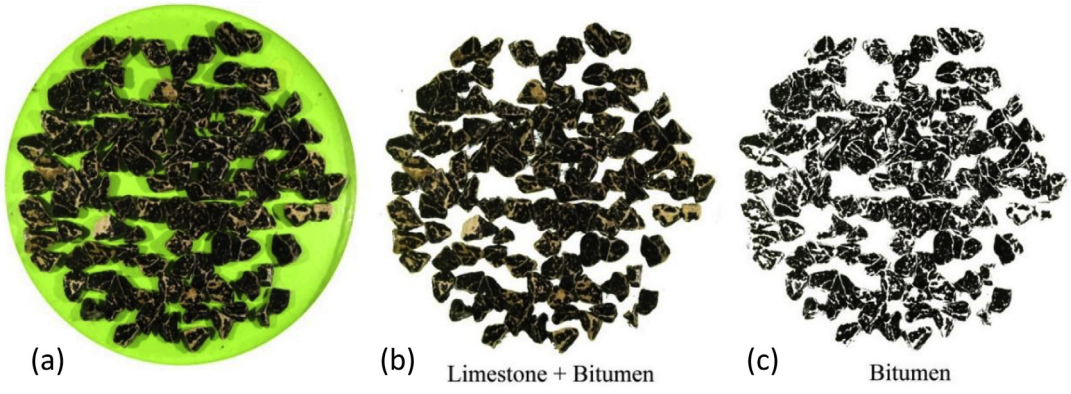

Fig. 2. Original image (a); non-classified image (b) and classified image (c).

Please cite this article in press as: C. Lantieri et al., Use of image analysis for the evaluation of rolling bottle tests results, Int. J. Pavement Res. Technol. (2016), http://dx.doi.org/10.1016/j.ijprt.2016.11.003

Table 1
Accuracy indexes for a matrix with k classes.

Overall Accuracy OA	Bitumen-Aggregate Accuracy BAA	k-th User Accuracy UA (k)	k-th Producer Accuracy PA (k)
$\frac{\sum_k P_{kk}}{\sum_{kj} P_{kj}}$	$\frac{\sum_{k=1}^{2} P_{kk}}{\sum_{k,j=1}^{2} P_{kj}}$	$\frac{P_{kk}}{\sum_j P_{kj}}$	$\frac{P_{kk}}{\sum_j P_{jk}}$

Table 2
Confusion matrix and accuracy index for limestone.

	Class	Reference data			Sum	User's Accuracy [%]
		L	Bit.	bkGD		
Classified image	L	204	17	2	223	91.5
	Bit.	5	529	8	542	97.6
	bkGD	0	0	1836	1836	100.0
Sum		209	546	1846	2601	
Producer's Accuracy [%]		97.6	96.9	99.5		

Table 3
Confusion matrix and accuracy index for porphyry.

	Class	Reference data			Sum	User's Accuracy [%]
		P	Bit.	bkGD		
Classified image	P	421	10	0	431	97.7
	Bit.	15	316	17	348	90.8
	bkGD	0	0	1822	1822	100.0
Sum		436	326	1839	2601	
Producer's Accuracy [%]		96.6	96.9	99.1		

Table 4
Confusion matrix and accuracy index for basalt.

	Class	Reference data			Sum	User's Accuracy [%]
		B	Bit.	bkGD		
Classified image	B	133	16	1	150	88.7
	Bit.	20	568	11	599	94.8
	bkGD	0	0	1852	1852	100.0
Sum		153	584	1864	2601	
Producer's Accuracy [%]		86.9	97.3	99.4		

than basalt (86.9%). This occurred because the classification method is based on the color: since the basalt is a dark aggregate, the contrast between bitumen and aggregate is low, raising the chances to fail with the classification [15,16].

Table 5 shows a summary of the Overall Accuracy (OA) and of the Bitumen-Aggregate Accuracy (BAA) indexes for all the adopted aggregates.

The OA index shows that the software is highly accurate. The BAA index indicates that the accuracy in recognizing the difference between the bitumen and the aggregate is greater than 95% for limestone, porphyry and basalt [15,16].

Table 5
OA and BAA indexes for the tested aggregates.

Aggregate	L	P	B
OA [%]	98.8	98.4	98.1
BAA [%]	97.1	96.7	95.1

3. Application of the procedure to wax modified binders

3.1. Materials

3.1.1. Aggregates

Three different aggregates were tested (Fig. 3):

- Basalt, mined in the region of Umbria, Italy.
- Limestone, mined in the region of Trentino-Alto Adige, Italy.
- Porphyry, mined in the region of Trentino-Alto Adige, Italy.

Please cite this article in press as: C. Lantieri et al., Use of image analysis for the evaluation of rolling bottle tests results, Int. J. Pavement Res. Technol. (2016), http://dx.doi.org/10.1016/j.ijprt.2016.11.003

Fig. 3. Basalt (a); limestone (b) and porphyry (c).

Table 6
Mixing temperatures corresponding to 0.17 Pa·s.

Base binder			
Temperature @ 0.17 Pa·s	135.7		
Wax 1 modified	1%	2%	3%
Temperature @ 0.17 Pa·s	131.2	130.5	129.9
Wax 2 modified	1%	2%	3%
Temperature @ 0.17 Pa·s	132.7	128.4	130.0

Besides being much employed in Italy, they were selected in order to cover a broad range of colors. All aggregates were washed and sieved to obtain an 8–11 mm fraction. Although EN 12697-11 [7] allows using also other fractions 6/10 and 5/8 mm, small fractions often results in a more difficult recognition as well as favoring the formation of clusters.

3.1.2. Binders

A 70/100 base bitumen was adopted. It was then modified with 1%, 2% and 3% by weight of two different waxes (W1 and W2) so that seven different binders were actually employed.

As one of the goals of this work is to assess the influence of the wax content on adhesion, the appropriate mixing temperature was chosen for each binder. As the wax reduces the viscosity of the bitumen, a change of the temperature is justified. An Anton Paar Dynamic Shear Rheometer was used to identify the temperatures at which each binder showed a viscosity of 0.17 Pa·s, as suggested by the Asphalt Institute's Superpave Level 1 Mix Design (SP-2).

A procedure proposed by Reinke [20], who describes an alternative methodology to the use of rotational viscometer to assess the viscosity of bitumen, was adopted. Amplitude sweeps, using 8 mm parallel plates and 1 mm gap, were carried out at five different temperatures (76, 82, 88 100 and 110 °C). The stress was varied from 0.33 to 500 Pa with gaps of 0.05 Pa.

Using an exponential regression, the mixing temperatures corresponding to the suggested viscosity were determined and are shown in Table 6.

It is evident that wax 1 is more effective at lower percentages, while wax 2 allows for a greater temperature reduction at 2% by weight of bitumen. However, both allowed reaching a temperature of 130 °C if mixed by the 3% (Figs. 4 and 5).

3.2. Procedure results

Table 7 shows the YUV ranges found for the image identification of the studied bituminous materials. Y, U and V can vary from 0 to 255. Lower or higher limits vary with different exposure conditions, i.e. with natural light, artificial light or both. In order to reproduce the analysis of the same materials, an operator could apply these YUV sets and easily obtain the non-classified and the classified images. For example, for the identification of the U parameter of limestone in the classified image, the lower limit is chosen between 80 and 100 and the upper limit is 255.

Once the YUV ranges were determined, the image analysis was carried out on the pictures taken of the

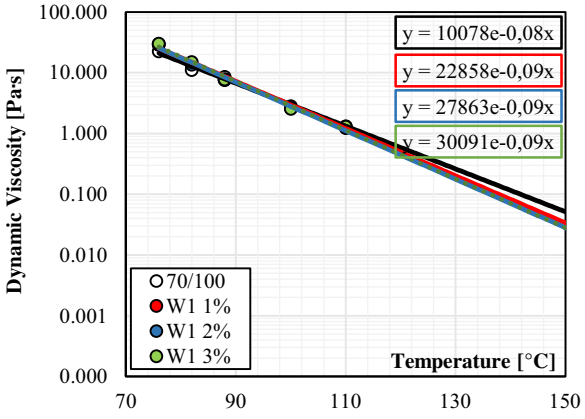

Fig. 4. Dynamic viscosity of 70/100 bitumen and 70/100 bitumen with 1%, 2% and 3% of wax 1.

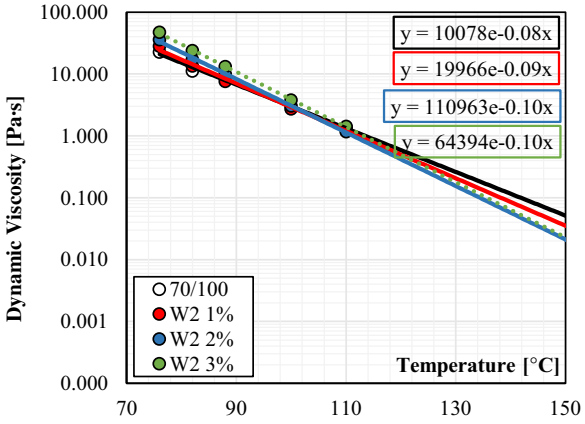

Fig. 5. Dynamic viscosity of 70/100 bitumen and 70/100 bitumen with 1%, 2% and 3% of wax 2.

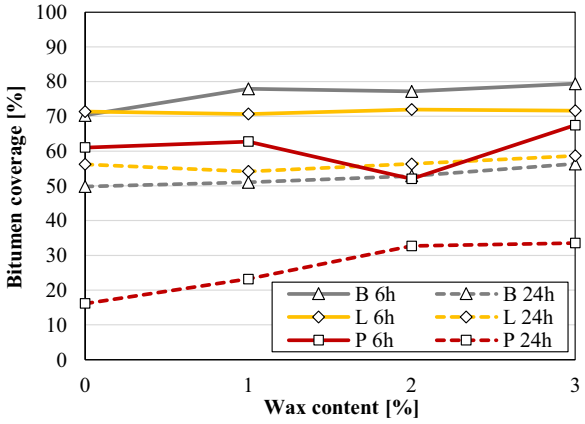

Fig. 6. Bitumen coverage versus wax 1 content.

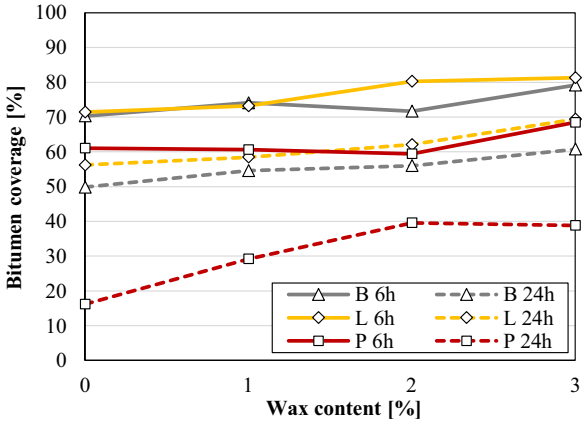

Fig. 7. Bitumen coverage versus wax 2 content.

investigated mixtures, according to the procedure described in 2.1.

Figs. 6 and 7 plot the bitumen coverage on the investigated aggregates versus the wax content in the bitumen, for waxes 1 and 2 respectively.

At a first glance the wax does not seem to affect the adhesion of the bitumen to the aggregates, which instead, mostly appears improved. Full and dashed lines indicate the results of the rolling bottle tests after 6 and 24 h of testing respectively.

In the case of wax 1, the more prominent effect is the enhancing of the adhesion bond of the porphyry at 24 h, which is doubled at 2% and 3% if compared to 0%. The basalt shows a slightly constant increase of the adhesion with increasing wax content, while the limestone does not show any significant change.

In the case of wax 2, the porphyry shows a very similar behavior compared to the case of wax 1, i.e. the wax strongly increases the adhesion with the bitumen, especially after prolonged rolling time. Both the basalt and the limestone exhibit a greater adhesion with the wax 2-modified bitumen compared to the base binder. The higher the wax 2 content the greater its positive contribute.

Using the same data, Figs. 8–10 compare the percentage of bitumen coverage obtained for the same aggregate mixed with the two different waxes. This highlights which wax affects the most performance in terms of adhesion. It is observed that, in all cases, wax 2 contributes to improve the bitumen-aggregate adhesion and its influence is greater than that offered by wax 1.

Looking at the aggregate performances, the more significant observation is the poor bitumen coverage of the porphyry both after 6 h and 24 h of rolling time. Porphyry group members are acid or intermediate igneous rocks and tend to be negatively charged. Aggregates containing large amounts of feldspar and quartz in crystals do not bind well with most of bitumens, which also has a slightly negative charge [19].

Despite this, porphyry could perform better with other binders or its adhesion being improved with the use of

Table 7
YUV ranges for materials' recognition.

		Basalt (B)	Limestone (L)	Porphyry (P)
Non-classified image	Y	0–165	0–195	0–165
	U	(90 ÷ 110) – 255	(80 ÷ 100) – 255	(80 ÷ 90) – 255
	V	(105 ÷ 120) – 255	(110 ÷ 120) – 255	(115 ÷ 120) – 255
Classified image	Y	0 – (25 ÷ 45)	0 – (55 ÷ 85)	0 – (25 ÷ 35)
	U	(90 ÷ 110) – 255	(80 ÷ 100) – 255	(80 ÷ 90) – 255
	V	(105 ÷ 120) – 255	(110 ÷ 120) – 255	(110 ÷ 120) – 130

Please cite this article in press as: C. Lantieri et al., Use of image analysis for the evaluation of rolling bottle tests results, Int. J. Pavement Res. Technol. (2016), http://dx.doi.org/10.1016/j.ijprt.2016.11.003

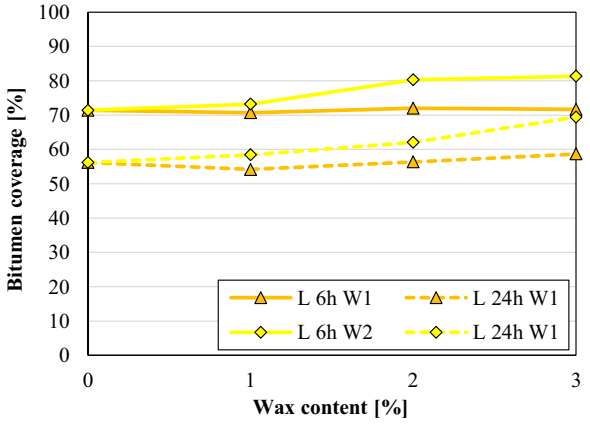

Fig. 8. Comparison between waxes 1 and 2 for Limestone.

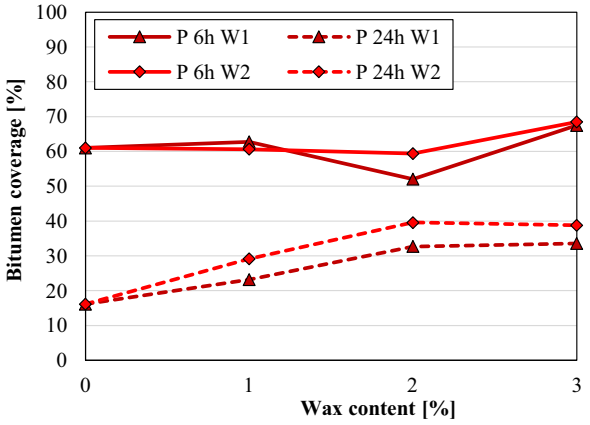

Fig. 9. Comparison between waxes 1 and 2 for Porphyry.

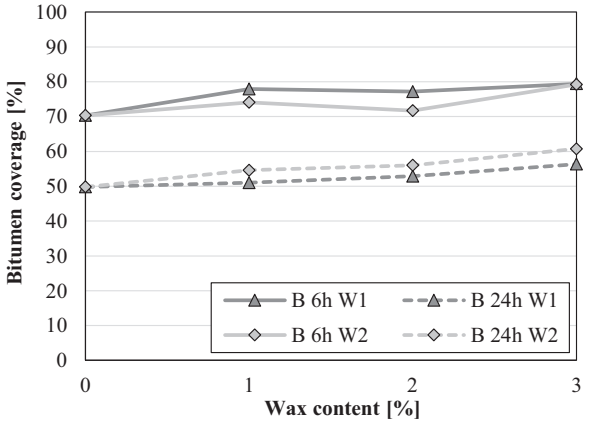

Fig. 10. Comparison between waxes 1 and 2 for Basalt.

adhesive agents. Basalt and aggregates exhibit similar good performances.

The wax 1-bitumen coverage is in the range of 70 ÷ 80% and 50 ÷ 60% after 6 h and 24 h of rolling respectively. The wax 2-bitumen coverage is in the range of 70 ÷ 80% and 50 ÷ 70% after 6 h and 24 h of rolling respectively.

After 6 h of testing, wax 1 performs better with the basalt, while wax 2 performs equally better with limestone and basalt. After 24 h of testing the limestone exhibits always greater bitumen coverage compared to the basalt, both in the case of waxes 1 and 2.

Table 8
Mean differences between visual and software estimations [%].

Binder	Limestone	Basalt	Porphyry
Base 70/100	13.54	−1.49	18.94
Wax 1 – 1%	3.43	4.06	19.59
Wax 1 – 2%	0.93	8.03	19.16
Wax 1 – 3%	6.00	13.82	22.57
Wax 2 – 1%	8.50	18.73	18.88
Wax 2 – 2%	10.02	9.99	25.12
Wax 2 – 3%	2.37	8.57	32.84
Average	6.4	9.2	22.4

3.3. Compliance with visual estimation

Three independent skilled operators carried out the visual recognition in order to verify the compliance with the computer aided procedure. Table 8 reports the differences between the degree of bitumen coverage determined with the software and the average of the visual recognition. The first was obtained as the average value of the results obtained on the three bottles for each mixture. The latter is the average value of the evaluation made by the three independent operators on the three bottles. It is observed that the operators tend to overestimate the bitumen coverage compared to the software recognition. Differences ranged from less than 1.00% to 32.84%.

Table 9 shows the standard deviations of both the visual and the software estimations. It is shown as on 18 out of 21 observations the standard deviation of the software is smaller compared to that of the visual estimate. This highlights a good reliability of the procedure, which helps minimizing outliers and giving similar results between observations.

4. Conclusions

Based on the proposed procedure and its application, the following can be summarized and concluded:

- the proposed procedure represents a fast and accurate method to assess the degree of bitumen coverage of aggregates after the rolling bottle test is performed. Its reliability and accuracy was validated through confusion matrices following pixel inspections of the images. The evaluation was found to be easier for light colored aggregates due to the contrast with the black color of the bitumen;

Please cite this article in press as: C. Lantieri et al., Use of image analysis for the evaluation of rolling bottle tests results, Int. J. Pavement Res. Technol. (2016), http://dx.doi.org/10.1016/j.ijprt.2016.11.003

Table 9
Standard deviations of the visual and software estimations.

	Limestone		Basalt		Porphyry	
	Visual St. Dev.	ImageJ St.Dev.	Visual St. Dev.	ImageJ St.Dev.	Visual St. Dev.	ImageJ St.Dev.
Base 70/100	3.42	1.63	3.14	2.05	1.36	2.00
Wax 1 – 1%	3.42	0.81	0.79	1.53	2.83	0.92
Wax 1 – 2%	4.16	2.42	2.08	2.28	1.57	0.71
Wax 1 – 3%	0.79	1.64	2.72	2.05	2.08	0.30
Wax 2 – 1%	4.16	0.77	6.80	0.87	3.60	1.49
Wax 2 – 2%	2.36	1.32	2.08	1.43	3.60	1.23
Wax 2 – 3%	1.57	1.21	3.42	1.81	2.72	1.59
Average	2.84	1.40	3.01	1.72	2.54	1.18

- the software estimation is, by far, more accurate compared to visual estimation. In fact, the standard deviation of the software results is smaller, demonstrating a low dispersion of the data;
- the divergences between visual and software recognition varied between 6.4% and 22.4%. For this reason, the first does not allow to make a consistent comparison between different aggregates and/or binders. On the contrary, the image analysis is an effective tool for the investigation and comparison of the affinity between different materials, as in the case of various percentages of waxes in a base binder.
- being the equipment quite simple and the software open source, this procedure is very cost-effective and may substitute or support the standard visual estimation. Furthermore, it would require less bottles to be tested, thus reducing the tested material as well as test and processing time;
- generally the adhesion between aggregate and bitumen improved with increasing the wax content compared to the adhesion obtained with the base binder. The entity of the improvement depends upon the wax and the aggregate.

References

[1] G.D. Airey, A.C. Collop, S.E. Zoorob, R.C. Elliott, The influence of aggregate, filler and bitumen on asphalt mixture moisture damage, Constr. Build. Mater. 22 (9) (2008) 2015–2024.
[2] A. Bhasin, Development of Methods to Quantify Bitumen-Aggregate Adhesion and Loss of Adhesion Due to Water, A&M University, Texas, 2006, Diss.
[3] A.C. Collop, Y. Choi, G.D. Airey, R.C. Elliott, Development of the saturation ageing tensile stiffness (SATS) test, Proc. Inst. Civ. Eng. Transp. 157 (3) (2004) 163–171.
[4] A.A. Cuadri, P. Partal, N. Ahmad, J. Grenfell, G.D. Airey, Chemically modified bitumens with enhanced rheology and adhesion properties to siliceous aggregates, Constr. Build. Mater. 93 (2015) 766–774.
[5] G. Dondi, A. Simone, V. Vignali, G. Manganelli, Discrete particle element analysis of aggregate interaction in granular mixes for asphalt: combined DEM and experimental study, Proceedings of 7th RILEM International Conference on Cracking in Pavements, June 20–22, Delft, The Netherlands, 2012.
[6] G. Dondi, V. Vignali, M. Pettinari, F. Mazzotta, A. Simone, C. Sangiorgi, Modeling the DSR complex shear modulus of asphalt binder using 3D discrete element approach, Constr. Build. Mater. 54 (2014) 236–246.
[7] EN 12697-11: Bituminous mixtures – Test methods for hot mix asphalt – Part 11: Determination of the affinity between aggregate and bitumen.
[8] EN 12697-12: Bituminous Mixtures – Test Methods for Hot Mix Asphalt – Part 12: Determination of the Water Sensitivity of Bituminous Specimens.
[9] C. Gorkem, B. Sengoz, Predicting stripping and moisture induced damage of asphalt concrete prepared with polymer modified bitumen and hydrated lime, Constr. Build. Mater. 23 (2009) 2227–2236.
[10] J. Grönniger, M.P. Wistuba, P. Renken, Adhesion in bitumen-aggregate-system: new technique for automated interpretation of rolling bottle test, Road Mater. Pavement Des. 11 (4) (2010) 881–898.
[11] A.W. Hefer, A. Bhasin, D.N. Little, Bitumen surface energy characterization using a contact angle approach, J. Mater. Civ. Eng. 18 (2006) 759–767.
[12] N.A. Ibraheem, M.M. Hasan, R.Z. Khan, P.K. Mishra, Understanding color models: a review, J. Sci. Technol. 2 (3) (2012).
[13] H. Källén, A. Heyden, K. Åström, P. Lindh, Measuring and evaluating bitumen coverage of stones using two different digital image analysis methods, Measurement 84 (2016) 56–67.
[14] R. Khan, J. Grenfell, A. Collop, G. Airey, H. Gregory, Moisture damage in asphalt mixtures using the modified SATS test and image analysis, Constr. Build. Mater. 43 (2013) 165–173.
[15] R. Lamperti, J. Grenfell, C. Sangiorgi, C. Lantieri, G. Airey, Influence of waxes on adhesion properties of bituminous binders, Constr. Build. Mater. 76 (2015) (2015) 404–412.
[16] R. Lamperti, C. Lantieri, C. Sangiorgi, G. Bitelli, A. Simone, Semi-automatic evaluation of the degree of bitumen coverage on bitumen-coated aggregates, 8th International RILEM Symposium, October 7–9, Ancona, Italy, 2015.
[17] J.S. Miller, W.Y. Bellinger, Distress Identification Manual for the Long-Term Pavement Performance Program, Publication FHWA-RD-03-031, FHWA, Virginia, 2003.
[18] C. Mulsow, Determination of the degree of gravel aggregate-bitumen coverage by multi-directional reflectance measurements, Paper presented at the XXII ISPRS Congress, Melbourne, 25 August–01 September 2012, 2012.
[19] C.A. O'Flaherty, Highways, Fourth Edition Elsevier – Technology & Engineering, 2002, p. 553.
[20] G. Reinke, Determination of mixing and compaction temperature of pg binders using a steady shear flow test, Superpave Binder Expert Task Group (2003), September 2003.
[21] V. Vignali, F. Mazzotta, C. Sangiorgi, A. Simone, C. Lantieri, G. Dondi, Rheological and 3D DEM characterization of potential rutting of cold bituminous mastics, Constr. Build. Mater. 73 (2014) 339–349.

Please cite this article in press as: C. Lantieri et al., Use of image analysis for the evaluation of rolling bottle tests results, Int. J. Pavement Res. Technol. (2016), http://dx.doi.org/10.1016/j.ijprt.2016.11.003

[22] V. Vignali, F. Mazzotta, C. Sangiorgi, A. Simone, C. Lantieri, G. Dondi, Incorporation of rubber powder as filler in a new dry-hybrid technology: rheological and 3D DEM mastic performances evaluation, Materials 9 (2016) 842–846.

[23] J. Zhang, A.K. Apeagyei, G.D. Airey, J.R.A. Grenfell, Influence of aggregate mineralogical composition on water resistance of aggregate–bitumen adhesion, Int. J. Adhes. Adhes. 62 (2015) 45–54.

Please cite this article in press as: C. Lantieri et al., Use of image analysis for the evaluation of rolling bottle tests results, Int. J. Pavement Res. Technol. (2016), http://dx.doi.org/10.1016/j.ijprt.2016.11.003